ISSN 0469-4732

INSTITUTE OF PLASMA PHYSICS

NAGOYA UNIVERSITY

$V_p \times B$ Acceleration – A New Mechanism of Particle Acceleration by Waves –

Ryo SUGIHARA

(Received – Apr. 24, 1987)

IPPJ- 830 May, 1987

RESEARCH REPORT

NAGOYA, JAPAN

$V_p \times B$ Acceleration - A New Mechanism of Particle Acceleration by Waves -

(Invited paper presented at the 1987 International Conference on Plasma Physics)

Ryo Sugihara

Institute of Plasma Physics, Nagoya University, Nagoya, Japan

ABSTRACT

A unique particle acceleration by an electrostatic (ES) wave, a magnetosonic shock wave as well as an electromagnetic (EM) wave is reviewed. The principle of the acceleration is that when a charged particle is carried across an external magnetic field the charge feels a DC field (the Lorentz force) and is accelerated. The theory for the ES wave acceleration is experimentally verified though it is semi-quantitative. The shock acceleration is extensively studied theoretically and in a particle simulation method and the application is extended to phenomena in interplanetary space. The EM wave acceleration is based on a trapping in a moving neutral sheet created by the wave magnetic field and the external magnetic field, and the particle can be accelerated indefinitely. A brief sketch on a slow-wave-structure for this acceleration will be given.

I. INTRODUCTION

When a finite amplitude electrostatic wave propagates across an external magnetic field perpendicularly, trapped particles moving with the wave feels a DC field (Lorentz force). Forslund-Morse-Nielsen claimed that this type of wave-particle interaction causes an anomalous resistivity in a plasma in which ions drift with respect to electrons [1] . Soon after, Sagdeev-Shapiro estimate an enhanced damping of the plasma wave due to this interaction in a weak magnetic field [2] .

If the number of the trapped particles is sufficiently small to keep the wave amplitude almost constant during the particle acceleration, then we may disregard the reaction of the particle motions to the wave field. This is realized if

$$\Pi_{tr}^2 \ll \Omega^2, \tag{1}$$

where $\Pi_{tr}^2 = 4\pi n_{tr} q^2/m$, $\Omega^2 = (qB/mc)^2$ and n_{tr} is the density of the trapped particles. I like to call the particle acceleration in such situation the $V_p \times B$ acceleration (more exactly " $V_p \times B$ acceleration by ES wave ") for abbreviation, where V_p stands for the phase velocity of the wave (including a shock) concerned. Sagdeev predicted in a text book that particles being reflected back by the electric field on the shock front may be accelerated along the shock front, repeating the bounce motion [3] . This may be the first argument on this unique acceleration stated in the present talk.

In an experiment of the turbulent plasma heating conducted in THE MACH II of IPP, Japan, it is found that the energies of impurity ions heated in the plasma are proportional to the masses of the impurities [4] . It is reasonable to think that the accelerated impurity ions are initially trapped in a large amplitude waves and accelerated by some mechanism. This unknown mechanism motivated us to look for a new mechanism which resulted in the $V_p \times B$ acceleration by ES waves [5] .

Just recently we have found that a transverse electromagnetic wave can also trap charged particles and accelerate them by the same principle. Important is that the energization of the particles is unlimited. I call this acceleration " the $V_p \times B$ acceleration by EM wave " and give a little detailed discussion on this work later on. We, however, call both cases simply the $V_p \times B$ acceleration as far as there occurs no confusion.

I here introduce several topics related to this new acceleration and emphasis will be put on those in Japan.

II. ACCELERATION BY LONGITUDINAL WAVES.

Imagine a situation shown in Fig.1 where no friction between the charge and the glass plate is assumed. If we push up the plate, the charged particle is forced to cross the magnetic field and feels a DC field f_x along the surface of the plate. And also a force pushing the plate, i.e., the y-component of the Lorents force, f_y, is present. A simple calculation gives us

$$f_x = qBV_p/c \equiv m\Omega V_p, \tag{2}$$

$$f_y = -m\Omega v_x = -m\Omega^2 V_p t, \tag{3}$$

$$v_x = V_p \Omega t, \tag{4}$$

where $v_{x0} \equiv v_x(0) = 0$ has been assumed. These three quantities represent our unique mechanism. The constant force f_x acts along the x-direction and therefore the velocity v_x increases in proportion to the time t while the force f_y pushing the plate also increases as t. If we replace the glass plate with the wall of the potential of an electrostatic wave, the wave only keeps the particle as long as the potential stands the increasing force f_y. When the force f_y overcomes the electrostatic force, then the particle detraps from the potential trough and makes a gyromotion essentially without gaining energy. This is the essence of the mechanism I am going to talk. The glass plate can be replaced with the shock but for a while we treat the case of the electrostatic wave.

The equation of motion is given by

$$md(\gamma\vec{v})/dt = (q/c)(\vec{v}\times\vec{B}) + q\vec{E}\sin(\vec{k}\vec{x} - \omega t), \tag{5}$$

where $\gamma = (1-v^2/c^2)^{-1/2}$ and other notations are standard. The amplitude $|\vec{E}|$ is supposed constant except for the shock wave in section II-4. It must be noted that during my talk the coordinates will be different from one work to another since I dare not to unify them because it is a little difficult.

II-1. θ-Dependence of Acceleration.

When θ is supposed to be the angle between the wave vector $\vec{k}$ and $\vec{B}$, the case of $\theta=\pi/2$ is first dealt with [5,6]. Also the case of $\theta \neq \pi/2$ is investigated and it is found that there is some optimum angle usually close to $\pi/2$ and the particle speed reaches $2V_E \equiv 2cE/B$, twice of that gained in the case of $\theta = \pi/2$ [7]. The direction of the maximum velocity is almost along $\vec{B}$. A relativistic treatment is also done and rigorous criterions for the unlimited acceleration (see II-3) for an arbitrary angle θ is obtained [8].

II-2. Experimental Verification of $V_p\times B$ Acceleration by ES wave.

II-2-1. Acceleration for $\theta = \pi/2$ [9].

The experiments are performed with a cylindrical nonuniform plasma produced in a 1 m long by 60 cm diameter chamber covered with multi-dipole magnets, as shown in Fig.2 where also the coordinates chosen are given. Now the wave term in Eq.(5) becomes $qE\vec{e}_z\sin(kz - \omega t)$, $\vec{e}_j$ being the unit vector along the j-axis ($j = x, y, z$). The typical plasma parameters produced by pulse discharges in Ar neutral gas are a maximum density of $n_e \simeq 2\times10^{11}\ cm^{-3}$, and an electron and ion temperature of $T_e \simeq 2.5 - 3$ eV and $T_i \simeq T_e/10 - 12$, respectively. A p-polarized electromagnetic wave with a frequency $f_0 = \omega_0/2\pi$ =2.45 GHz and maximum power $P\simeq$ 3.5 kW ($\simeq$ 14W/cm^2) is launched along the density gradient from a high-gain horn antenna. The magnetic field, less than 11 G, produced by two coils outside the chamber is applied vertically (y-direction) to the density gradient as seen in Fig.2. In a higher density region than the reflection point, an electrostatic plasma wave is excited at the critical layer with frequency ω_0. This wave travels down the density gradient a few centimeters with a wavelength of about 0.2 - 0.5 cm.

When the rf wave is launched, even without a magnetic field a high energy electron component of about 35 - 40 eV is produced by the transit time acceleration due to the localized electric field. When a weak magnetic field is applied, the energy of the high energy component in the x-direction increases to about 90 eV. A further increase of the magnetic field again reduces the maximum energy of the high energy electron component. The dependence of the magnetic field is shown in Fig.3. Note that the particle energy ε decreases as B^{-2} for $B > 3$G. This tendency is explained by the fact that the particle energy will be given by

$$\varepsilon = \varepsilon_0 + (m/2)(E/B)^2,$$

where ε_0 is the initial value of ε. The increase for $B \lesssim 3$ G is due to some other cause (see Ref.9).

When we change the polarity of the magnetic field, keeping its intensity constant, the electron energy changes drastically, as shown in Fig.4. In this example, " toward " means that only the electrons emitted out in the direction " $(-e)\vec{V}_p\times\vec{B}$ " are collected, and " opposite " stands for the reversed direction. It is clearly seen that the electrons are accelerated only in the direction " $(-e)\vec{V}_p\times\vec{B}$ ", not in the opposite direction. It is confirmed that hot electrons are ejected from narrow regions of width $\cong$ 1.0 - 1.5 cm located near and at a slightly lower density region than the critical layer as shown in Fig.5. We also show the RF electric field distribution for comparison purposes. Since the trapped particles must be carried away by the longitudinal wave before the ejection, the concerning peak position of the electron emission should be separated from the peak at the critical layer z_c. The small spatial separation Δz between two peak positions of the electron energy is measured as a function of the RF irradiation power, P, which is also shown in the inset of Fig.5. The solid line in the inset is a prediction of the theory. These results are consistent with the theory [5].

II-2-2. Acceleration for $\theta \neq \pi/2$ [10].

Using the same device Nishida et al. reveal that a large amplitude electrostatic wave propagating obliquely to the magnetic field strongly accelerates electrons almost along the magnetic field line. The experimental conditions are the same as those in II-2-1 except for the magnetic field, which is now non-uniform and makes a weak mirror as seen in Fig.6. The ES wave propagates down the density gradient and its wave front is almost parallel to the equi-density line. When we shift up the critical layer z_c along the z-axis, the propagation angle θ changes between

$30^\circ \leqq \theta \leqq 90^\circ$ (in $x \neq 0$ area) because of the bending of the magnetic field lines while the mgnetic field strength does not change in the y-direction within this experimental area. Changing the z_c or θ, we measured maximums of high energy electron fluxs I_{hx} (denoted as I_{hx}^{p}). The I_{hx}^{p} vs. θ is shown in Fig.7. We see a clear peak around a critical θ, θ_c, the presence of which is predicted in the theory [7] .

II-3. Unlimited Acceleration and Surfatron Accelerator.

In Eq.(5), $\vec{B}$ is now taken to be along the z-axis and the wave term is $qE\vec{e}_x \sin(kx - \omega t)$. In the limit of relativistic velocity, the second term on the right hand side of (5) can be always larger than the first term if $E > \gamma_p B$ where $\gamma_p = (1 - V_p^2/c^2)^{-1/2}$. And in this case the particle can not detrap from the wave potential and be accelerated indefinitly. This is the principle of the Surfatron accelerator proposed by Katsouleas-Dawson [11] . A detailed discussion on this topic has been given elsewhere [12] .

II-4. Acceleration by a Magnetosonic Shock Wave.

As is stated in section I a possibility of the acceleration by a shock wave has been predicted [3] . Ohsawa extensively study this topic theoretically and also in particle simulation method. Here some of his works are presented.

A 2-1/2 dimension, fully relativistic, fully electromagnetic particle code is used to study the time evolution of a nonlinear magnetosonic pulse propagating in the x-direction perpendicular to the magnetic field directing in the z-axis. The pulse is excited by an instanteneous piston acceleration and evolves in a totally self-consistent manner. In Fig.8, ion phase space plots for the weak pulse [(a) and (b)] and for the strong pulse [(c) – (f)] are shown. For the weak pulse with the

B_m(maximum B)/B_1(upstream B) = 1.17, no resonant ions are found. For the strong pulse with B_m / B_1 = 1.75, a large number of high energy ions are generated by $V_p \times B$ acceleration mechanism [13].

Next I will show you the case of high Alfven velocity v_A, i.e.,

$$c > v_A \gtrsim c(m_e/m_i)^{1/2}.$$

Ohsawa predicts that the motion of the resonant particles becomes relativistic though v_A is not close to c. In the simulation, he uses c = 4 and v_A = 1.2. Results are shown in Fig.9. For a high Mach number, M = 1.83, the resonant ions are accelerated up to a relativestic velocity and also the electrons get a relativistic energy [14].

Finally, it is commented that the $V_p \times B$ acceleration can be used to interprete phenomena in interplanetary space. One example is the interpretation of the observations of Voyager II [15] which observed unexpectedly high energy ions in association with a quasi-perpendicular magnetosonic shock wave with the propagation angle θ = 87.5° at a distance of 1.9 AU from the Sun. The theory explains the following important features of the observation; 1) protons with energy $\gtrsim 10^6$ eV can be produced by a low-Mach-number interplanetary shock, 2) the kinetic energy increases with ion masses, 3) the acceleration is extremely strong in nearly perpendicular shocks with the propagation angles in the region 88.7° ± a few degrees [16].

III. ACCELERATION BY ELECTROMAGNETIC WAVE.

We here show that an electromagnetic wave with a purely transverse electric field can trap charged particles and accelerate them ($V_p \times B$ acceleration by EM wave). Characteristic is that the trapped particles never detrap and are accelerated indefinitely unless the wave is depleted[17,18] .

We assume that the wave electric field $\vec{E}$, the wave magnetic field $\vec{H}$, $\vec{k}$ and the static field $\vec{B}$ have components, $\vec{E} = (E_x, 0, 0)$, $\vec{H} = (0, 0, H_z)$, $\vec{k} = (0, k, 0)$ and $\vec{B} = (0, 0, B)$, respectively. We also assume that the phase velocity V_p is a little slower than the light velocity c. It may be paradoxical that the slow wave does not have any H_y component. Discussion on a more consistent wave field will be given later on. The equation of motion will then be

$$md(\gamma v_x)/dt = qE_x + (qv_y/c)(B + H_z), \tag{6}$$

$$md(\gamma v_y)/dt = -(qv_x/c)(B + H_z). \tag{7}$$

We assume that E_x and H_z have the forms $(E_x, H_z) = (E, -H)\cos(ky - \omega t + \alpha)$, α being the phase angle, and E and H are related each other through the refractive index N, i.e.,

$$N = c/V_p = H/E. \tag{8}$$

In the wave frame where quantities are identified in capital letters, Eqs.(6) and (7) write

$$d(\Gamma V_x)/dT = \gamma_p V_p \Omega + (qV_y/mc)B(Y), \tag{9}$$

$$d(\Gamma V_y)/dT = -(qV_x/mc)B(Y), \tag{10}$$

$$B(Y) = \gamma_p B - \gamma_p^{-1} H\cos(KY + \alpha), \tag{11}$$

where (8) was used and $K = k\gamma_p^{-1}$, $\Omega = qB/mc(>0)$,

$\Gamma = [1 - (V_x^2 + V_y^2)/c^2]^{-1/2}$.

We show semi-quantitatively that the particle can be trapped in the vicinity of the points where $B(Y) = 0$ and the momentum along the x-axis increases with the time T. Suppose the particle be trapped near some points where $B(Y) = 0$. Choosing the phase angle α so that $B(0) = 0$, and expanding $B(Y)$ around $Y = 0$, we have $B(Y) \doteqdot \gamma_p^{-1} \cdot (KY) \cdot H \cdot \sin\alpha$. The solution to Eq.(9) is approximately given by

$$\Gamma V_x = \Gamma_0 V_{x0} + \gamma_p V_p \Omega T + \Omega_H (\sin\alpha/K) [(KY)^2 - (KY_0)^2] , \tag{12}$$

where $\Omega_H = qH/mc\gamma_p$,and Y_0, V_{x0} and Γ_0 are the initial values of the corresponding values, and V_{x0} is assumed positive. We also assume that $\Gamma K V_{x0} > \Omega_H$ and hence the right hand side of Eq.(12) can be approximated by

$$\Gamma V_x = \Gamma_0 V_{x0} + \gamma_p V_p \Omega T. \tag{13}$$

Substituting this and the relation $B(Y) = \gamma_p^{-1} \cdot H \cdot (KY) \cdot \sin\alpha$ into Eq.(10) we get

$$\Gamma d(\Gamma V_y)/dT = -\omega_B^2 [1 + (\gamma_p V_p / \Gamma_0 V_{x0}) \Omega T] Y, \tag{14}$$

where $\omega_B^2 \equiv \Gamma_0 K V_{x0} \Omega_H \sin\alpha$ is assumed positive. We change T into τ by the transformation $d\tau = \Gamma^{-1} dT$ and then Eq.(10) becomes

$$d^2Y/d\tau^2 = -\omega_B^2 \cdot \psi(\tau) \cdot Y, \tag{15}$$

where $\psi(\tau) \equiv 1 + (\gamma_p V_p / \Gamma_0 V_{x0}) \Omega T(\tau)$. This equation represents a simple harmonic oscillator with an increasing mass and the orbit of the particle, while oscillating, converges to the point $Y = 0$. The approximation (13) is thus guaranteed. In the above calculation we have assumed $B(0) = 0$. This assumption is equivalent to the statement that the total magnetic field

$B(Y)$ has neutral points in one dimensional space or neutral sheets in three dimensional space, and the calculation shows that the test particle can be trapped in anyone of the neutral points(sheets) where $\sin\alpha > 0$. These arguments lead to the condition that, in order for a particle to be trapped, the relation

$$H > \gamma_p^2 B, \tag{16}$$

or

$$E > \gamma_p^2 B, \tag{17}$$

must hold where $H = NE \fallingdotseq E$ was used.

The trapped particle gains energy through the relation

$$mc^2 d\Gamma/dT = m\gamma_p V_p \Omega V_x, \tag{18}$$

which is easily obtained from Eqs.(9) and (10). Using Eq.(13) we find that the energy increases in the limit of $T \to \infty$ as $mc^2\Gamma = mc\gamma_p V_p \Omega T$, which can be rewritten as

$$mc^2\gamma \fallingdotseq mc\gamma_p V_p \Omega t, \tag{19}$$

by using $\gamma = \Gamma\gamma_p(1 + V_p V_y/c^2) \fallingdotseq \Gamma\gamma_p$ and $t = \gamma_p(T + V_p Y/c^2) \fallingdotseq \gamma_p T$. Equation (19) implies that the energy of the trapped particle increases proportionally to the time t. Figure 10 shows the time evolutions of the velocity component v_y and γ in the laboratory frame calculated numerically by using Eqs.(6) and (7). The γ follows the prediction of Eq.(19) and the behavior of v_y indicates that the particle centers on $Y = 0$. Thus, as (19) indicates, the trapped particle never detraps and is accelerated unlimitedly.

So far we have assumed the existence of a slow wave which couples with the particles. An example of slow waves is a wave propagating inside a parallel waveguide whose walls are composed of dielectric materials as shown in Fig.11. We choose a TE mode which has components, $E = [\ E_x(y,\ z),\ 0,\ 0\ ]$, and $H = [\ 0,\ H_y(y,\ z),\ H_z(y,\ z)\ ]$ and the z-dependence of the components is $(E_x, H_z) = (E, -H)\cosh(\kappa z)\cos(ky - \omega t + \alpha)$ and $H_y(y,\ z) = (\kappa/k)H\sinh(\kappa z)\sin(ky - \omega t + \alpha)$, where $\kappa \doteqdot k(N-1)^{1/2}$ if $N - 1 \ll 1$, N being the refractive index of the dielectrics.

The motion of the trapped particle will be unstable due to the presence of $H_y(y,z)$. Assume that we are able to superpose a sheared steady field $H_s \equiv h \cdot (\kappa z)\vec{e}_y$. Let us analyse the stability to small deviations $|\ KY\ | \ll 1$, and $|\ \kappa z\ | = |\ \kappa Z\ | \ll 1$ from the origin around which the motion would be stable if $\kappa = 0$. We have two independent equations, one is given by Eq.(15) and the other is

$$d^2Z/d\tau^2 = b_y \cdot \omega_\xi^2 \cdot \psi(\tau) \cdot Z, \tag{20}$$

where $b_y \equiv (\kappa/K)\ [\kappa/K + h/(H\sin\alpha)]$. The orbit may become unstable to a perturbation along the z-axis if $h = 0$, since $kK > 0$ and $\omega_\xi^2 > 0$, a necessary condition for the stability along the y-axis(see (15)). So if we can choose $h/H < 0$ and $|\ h/H\ | > (\kappa/k)\sin\alpha$ the motion will be stable to the perturbation. For example when $N - 1 = 10^{-2}$, we have $\kappa/k \doteqdot 10^{-1}$ and $|\ h\ |$ of one-tenth of H is enough for keeping stability.

We compare characteristic features of the present scheme with those of the unlimited acceleration by the electrostatic wave. The results are given in Table I. Predominant differences are the following. In the case of the electrostatic wave a two-laser-beat-wave creates a slow mode with a very steep gradient field in the plasma though the plasma control is a big problem. In the present scheme a high power microwave is the first candidate for the driver wave. In near future a free-electron-laser with a relatively long wavelength may be utilized as the driver.

IV. CONCLUSIONS.

I here presented a brief survey of a unique mechanism of particle acceleration, i.e., $V_p \times B$ acceleration. First we discussed the acceleration by electrostatic waves including a shock wave. A particle carried by the wave or pushed by a shock wave across a static magnetic field feels a DC field (Lorentz force) and is accelerated. If $E > \gamma_p B$, the particle is accelerated indefinitely. It is found that the particle gets more energy than that for $\theta = \pi/2$ if the propagation angle θ, where $\theta = \angle \vec{k}, \vec{B}$, takes a proper value a little less than $\pi/2$. This acceleration scheme was verified experimentally for both $\theta = \pi/2$ and $\theta \neq \pi/2$ by using a Langmuir wave. Study on this acceleration by a magnetosonic shock wave is extensively done by a 2-1/2 dimension particle simulation and is applied to interprete phenomena in interplanetary space. A quite new feature of the acceleration, an acceleration by a transverse electromagnetic wave, is presented. It is found that a particle can be trapped by a TE mode and that it is energized indefinitely. Characteristic features are compared with those of the unlimited acceleration by the electrostatic wave.

Acknowledgements

I am very much indebted to Drs. Y. Nishida, and Y. Ohsawa for thier contributions in preparing the talk.

References

1) D. Forslund, R. Morse and C. Nielsen, Phys. Rev. Lett. 27 (1971) 1424.

2) R.Z. Sagdeev and V. Shapiro, Pis'ma Zh. Eksp. Teor. Fiz. 17 (1973) 389 [JETP Lett. *Vol*.17 (1973) 279] .

3) R.Z. Sagdeev, in Reviews of Plasma Physics, Vol.4, edited by M.A. Leontovich (Consults Bureau, New York, 1964) p.76.

4) K. Adati, H. Iguchi, Y. Ito, T. Kawabe, K. Kawasaki. T. Oda, R. Sugihara and T. Yokota, in Proc. 7th Europ. Conf. Controlled Fusion and Plasma Physics, Lausannes, 1975 , Vol.1, p.166.

5) R. Sugihara and Y. Midzuno, J. Phys. Soc. Jpn, 47 (1979) 1290.

6) J.M. Dawson, V.K. Decyk, Robert W. Huff, I. Jechart, T. Katsouleas, K.N. Leboeuf, B. Lembege, R.M. Martinez, Y. Ohsawa, and S.T. Ratliff, Phys. Rev. Lett., 50 (1983) 1455.

7) R. Sugihara, S. Takeuchi. K. Sakai and M. Matsumoto, Phys. Rev. Lett., 52 (1984) 1500.

8) K. Sakai, S. Takeuchi, M. Matsumoto, research report of Institute of Plasma Physics, Nagoya University, IPPJ-680, May 1984.

9) Y. Nishida, M. Yoshizumi and R. Sugihara, Phys. Fluids 28 (1985) 1574.

10) Y. Nishida, N.-Y. Sato, private communication.

11) T. Katsouleas and J.M. Dawson, Phys. Rev. lett. 51 (1983) 392.

12) J.M. Dawson, in Proc. Int. Conf. Plasma Physics, Lausannes, 1984, Vol.2, p.837.

13) Y. Ohsawa, Phys. Fluids, 28 (1985) 2130.

14) Y. Ohsawa, J. Phys. Soc. Jpn, 55 (1986) 1047.

15) E.T. Sarris, S.M. Krimigis, Ap. J., 298 (1985) 676.

16) Y. Ohsawa, IPPJ-808, Dec. 1986 and also Geophys. Res. Lett., in press.

17) S. Takeuchi, K. Sakai, M. Matsumoto and R. Sugihara, IPPJ-740, July

1984 and also Phys. Lett., to be published.

18) S. Takeuchi, K. Sakai, M. Matsumoto and R. Sugihara, IEEE Trans. Plasma Sci. PS-15 (1987), in press.

Table Caption

Table I Characteristic features of the electromagnetic-wave-acceleration and of the unlimited acceleration by the electrostatic wave(Surfatron).

Figure Captions

Fig.1 Orbit of a charged particle which is on a friction-less glass plate.

Fig.2 Schematic description of the experimental apparatus. In the real system, a probe system is turned 90°. The distance between two probes is variable from the outside.

Fig.3 The dependence of ε and I_h, the electron current flux with energy more than 60 eV, on B. $P \cong 800$ W.

Fig.4 Effect of polarity of the magnetic field on the energy distribution. I_p is the probe current.

Fig.5 The total RF electric field strength $|E^2|$, and the maximum energy of the high energy component versus the axial position observed at $P \cong 1.3$ kW and $B = 3.5$ G. Inset shows the spatial difference Δz observed between two peaks of ε versus the square root of the normalized input power at $P_0 = 1$ kW.

Fig.6 Schematic description of the oblique propagation of ES wave with angle θ to the magnetic field lines.

Fig.7 The maximum of high energy electron flux, I_{hx}^{*}, (open circles) versus the propagation angle θ. " θ_c " shows the optimum angle. The solid line indicates the theoretically estimated v_T. Inset shows the optimum angle θ_c versus the square root of RF power normalized by P_0 = 1 kW at $B_0 = -5$ G. Again the solid line shows the theoretical prediction.

Fig.8 Ion phase space plots for weak pulse((a) and (b)), and for strong pulse ((c)-(f)). For strong pulse with B_{m}/B_{1} = 1.75, a large number of high energy ions are generated.

Fig.9 Phase space plots ($p_{xj}/m_{j}c$, $p_{yj}/m_{j}c$) for the ions ((a)-(c)) and electrons ((d)-(f)). (a) and (d) are the phase space plots in the upstream region. The others are those in the downstream region for the shocks with M_A = 1.37 ((b) and (d)) and M_A = 1.83 ((c) and (f)).

Fig.10 The time evolutions of the velocity v_y and γ of a trapped electron. v_y gradually converges to the phase velocity V_p. The kinetic energy $mc^2\gamma$ increases indefinitely. The parameters are specified as V_p/c = 0.85, E/B = 6.9 and v_{x0}/c = 0.2.

Fig.11 Schematic diagram of the slow-wave-structure. The static magnetic field $\vec{B}$ is applied perpendicular to the wall. TE-mode wave propagates in the y-direction. An electron beam is injected perpendicular to the z-axis and obliquely to the y-axis.

TABLE I

	Present Scheme	Surfatron
Trapping time	Unlimited	Unlimited
Driver	Electromagnetic Wave	Electrostatic Wave
Plasma	Not Necessary	Necessary
γ	$\gamma_p{}^2\Omega V_p\, x / c^2$	$\gamma_p{}^2\Omega V_p\, x / c^2$
$\Delta\gamma / \gamma$	Converging	Converging
Condition on E and B	$E_x > \gamma_p{}^2 B$	$E_y > \gamma_p B$

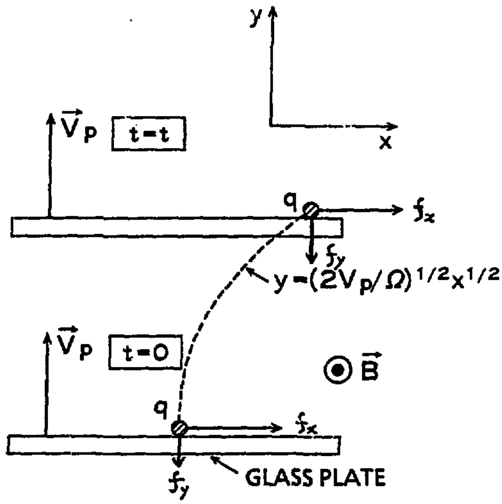
y
x
$\vec{V}_P$
t=t
q
f_x
f_y
$y=(2V_P/\Omega)^{1/2}x^{1/2}$
$\vec{V}_P$
t=0
$\vec{B}$
q
f_x
f_y
GLASS PLATE

FIG.1

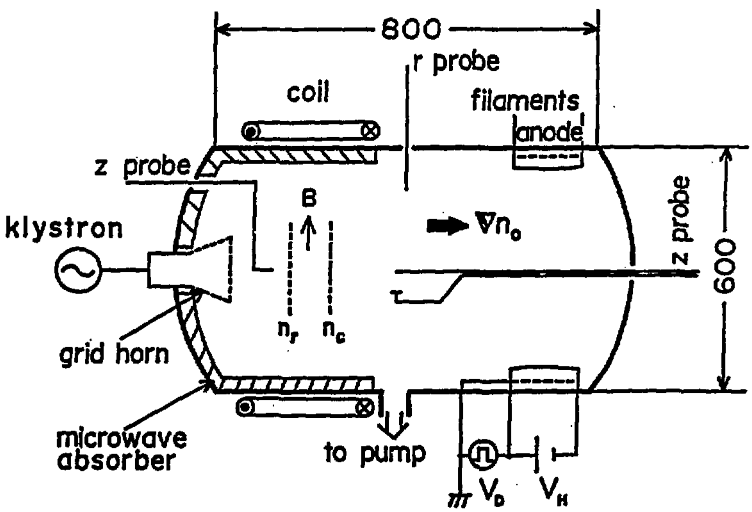
800
r probe
coil
filaments
anode
z probe
B
∇n_0
klystron
z probe
600
n_r
n_c
grid horn
microwave absorber
to pump
V_D
V_H

FIG.2

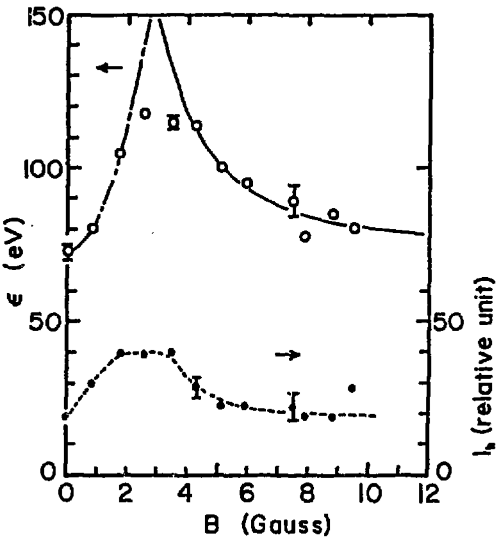
150
100
50
0
50
0
ε (eV)
I_s (relative unit)
0
2
4
6
8
10
12
B (Gauss)

FIG.3

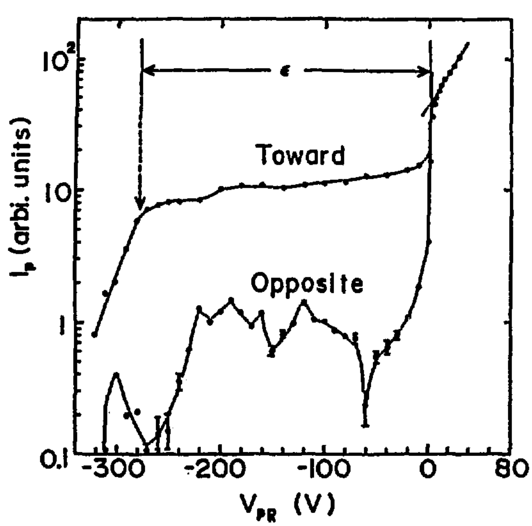
10^2
10
1
0.1
ε
Toward
Opposite
I_p (arbi. units)
-300
-200
-100
0
80
V_{PR} (V)

FIG.4

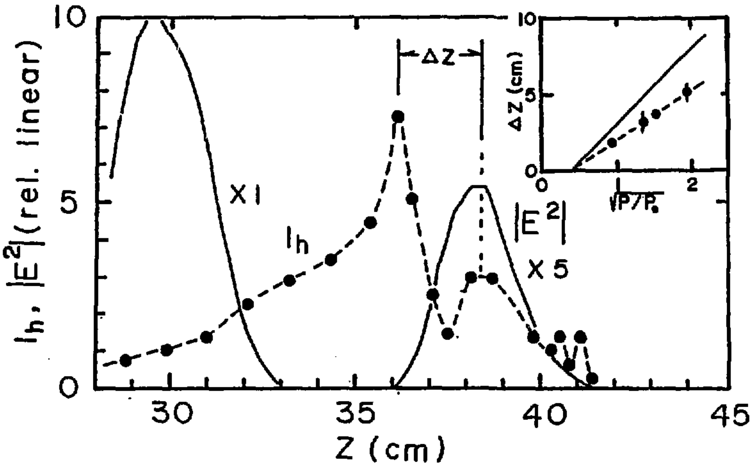

10
5
0
30
35
40
45
Z (cm)
I_h, $|E^2|$(rel. linear)
X1
I_h
ΔZ
$|E^2|$
X 5
10
5
0
0
1
2
ΔZ (cm)
$\sqrt{P/P_o}$

FIG.5

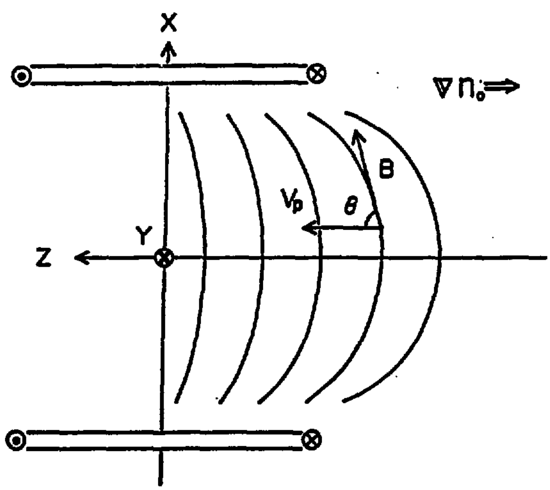

X
∇n_o
B
V_p
θ
Y
Z

FIG.6

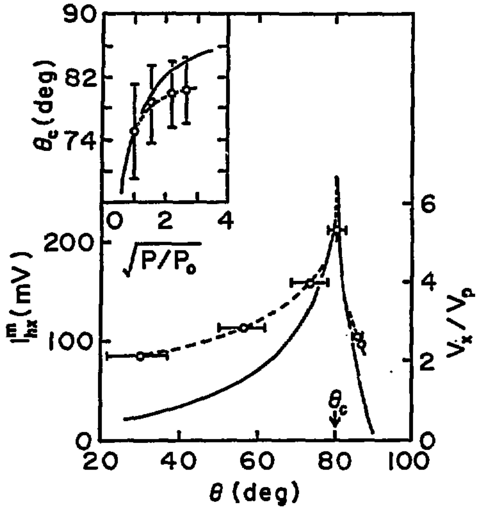

90
82
74
θ_c (deg)
0
2
4
$\sqrt{P/P_o}$
200
100
0
I^m_{hx} (mV)
6
4
2
0
V_x/V_p
θ_c
20
40
60
80
100
θ (deg)

FIG.7

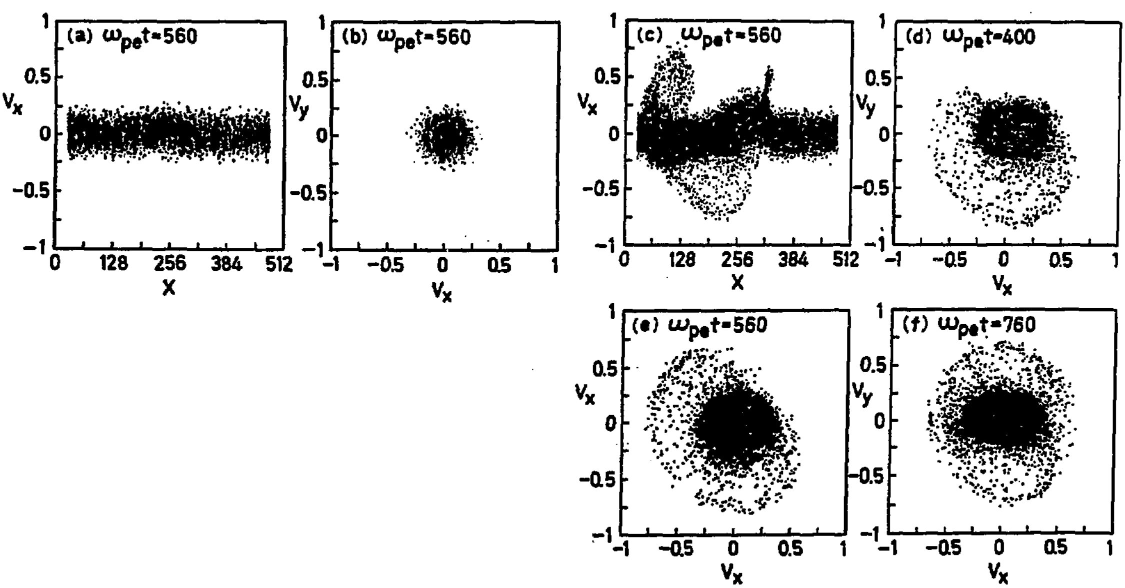

(a) $\omega_{pe}t$=560
(b) $\omega_{pe}t$=560
(c) $\omega_{pe}t$=560
(d) $\omega_{pe}t$=400
(e) $\omega_{pe}t$=560
(f) $\omega_{pe}t$=760
V_x
V_y
X
0
128
256
384
512
-1
-0.5
0
0.5
1

FIG.8

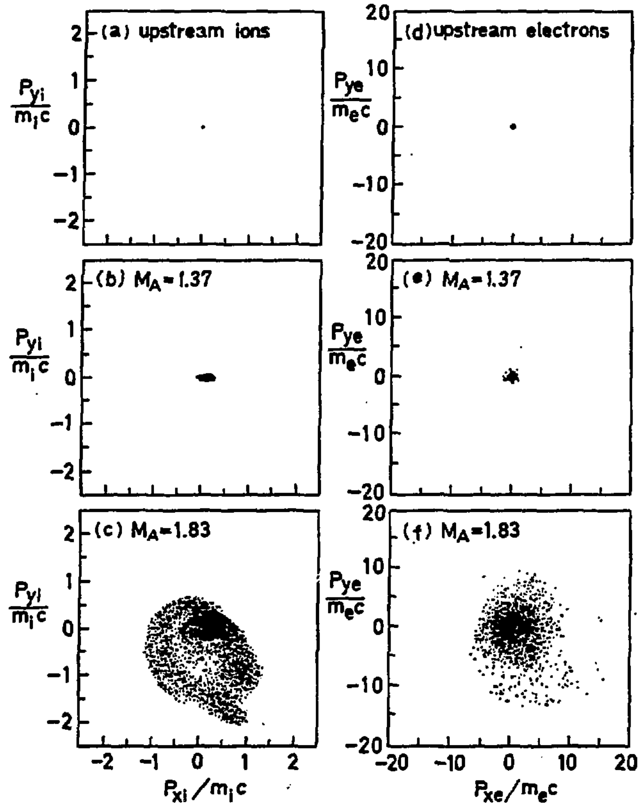
(a) upstream ions
(b) M_A=1.37
(c) M_A=1.83
(d) upstream electrons
(e) M_A=1.37
(f) M_A=1.83
$P_{yi}/m_i c$
$P_{ye}/m_e c$
$P_{xi}/m_i c$
$P_{xe}/m_e c$

FIG.9

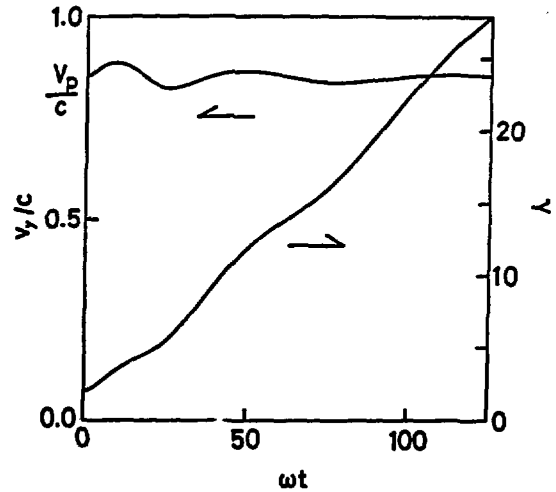
V_p/c
v_y/c
γ
ωt

FIG.10

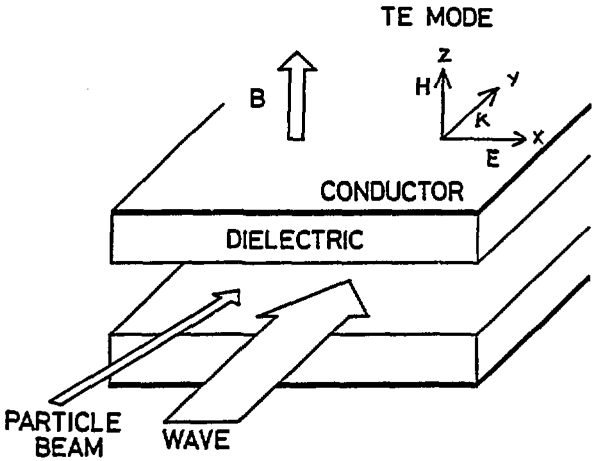

FIG.11